Appendix 1 Supplementary Method

Establishment and validation of ML models

In the initial stage of model establishing, the Least Absolute Shrinkage and Selection Operator (Lasso) was used to select variables. Our purpose was to identify the features most closely related to RP-ILD diagnosis in patients with IIM-ILD, for our subsequent ML modeling. We specifically chose the Lasso model for QCT features selection to address collinearity and to remove redundant or unmeaningful information provided by the software.

Firstly, we carefully examined the presence of any missing values in the entire dataset of all QCT attributes (table available at https://cdn.amegroups.cn/static/public/qims-24-595-1.xlsx). Features with more than 5% missing value were then eliminated (table available at https://cdn.amegroups.cn/static/public/qims-24-595-2.xlsx). To substitute the missed value in the retained QCT features, we applied a mean interpolation process. For ensuring that the data distribution remained consistent before and after interpolation, we compared the QCT feature distribution both before and after the interpolation (table available at https://cdn.amegroups.cn/static/public/qims-24-595-3.xlsx). Next, we retained all characteristics with a variance that was greater than zero (table available at https://cdn.amegroups.cn/static/public/qims-24-595-4.xlsx). In our opinion, a variance of zero illustrated that the features were entirely consistent across all patients and therefore, have no significant value for classification models. Finally, after normalizing the data, a Lasso regression model was established in random 70% data as a train set, and we calculated the mean squared error in the test set (30%) for optimization. The lambda parameter was also optimized using a 5-fold cross-validation in the train set (Figure S1) and the least mean squared error in the test set. We preserved the features whose Lasso coefficients were not eliminated (Table S1).

In the second phase, we implemented eight widely practiced machine learning approaches including Naive Bayes, Logistic Regression, K-Nearest Neighbors, Random Forests, Decision Trees, Gradient Boosting Trees, Support Vector Machines, and Multilayer Perceptron (specific parameters in the Appendix 1). For each model, the overall dataset was randomly partitioned into train and test sets in a 7:3 ratio. Next, we trained the models on the train set and utilized 5-fold cross-validation with grid search to identify the most favorable parameters. To evaluate the efficiency and performance of the models, we derived confusion metrics to calculate accuracy, sensitivity, specificity, precision, F1 score, positive predictive value, negative predictive value, Jacobian index, net reclassification index (NRI), integrated discrimination improvement (IDI), and the AUC (area under the curve) for the ROC (receiver operating characteristic) curve in the test set. Furthermore, we plotted the ROC for each model. By executing this stage, our primary objective was to identify the most outstanding and explainable ML model that predicts the RP-ILD diagnosis based on QCT features.

With the selected ML approach, we included both clinical data and QCT features to build the final model. Specifically, we only included cases with complete clinical and HRCT information and adopted a 7:3 scheme to randomly divide the train and test sets. As the GGOs and consolidation features in HRCT are often considered to be related to RP-ILD outcomes, we specified that the model must incorporate QCT features related to GGOs and consolidation. Similarly, DL_{CO} percentage, FEV_1 percentage, and OI are clinical indicators known to be related to RP-ILD, and we also specified that the model must include these indicators.

For the final model evaluation, we used the accuracy, sensitivity, specificity, precision, F1 score, positive predictive value, negative predictive value, Jacobian index, and the AUC based on the prediction value generated from the logistic regression model. Furthermore, we compared the performance differences between the only clinical model, the only HRCT model, and the final combined model using ROC plot, NRI, and IDI. Additionally, we drew calibration curves, nomograms, and clinical decision-making curves to further evaluate the application potentials of the model.

Model parameters

Naive Bayes

The algorithm calculates the conditional probabilities of the class outcomes (RP-ILD and non-RP-ILD) given the prior information represented by the priori parameters. The 'naive' element of the algorithm refers to its assumption of independence among predictor variables. Nevertheless, since these parameters tend to be interdependent in actual practice, the estimated conditional probabilities may not always be entirely accurate. We utilized the 'naive_bayes' function from the

 https://dx.doi.org/10.21037/qims-24-595

'naivebayes' package to establish the model, selecting the parameters 'laplace' was 0, 'usekernel' was False, and adjust was 0, while leaving other parameters at their default values.

Logistic regression

Since logistic regression is designed for binary-dependent variables, RP-ILD and non-RP-ILD types of patients in the dataset were replaced with 1 and 0, respectively. We employed the 'glm' function from the 'stats' package, in combination with the 'step' function in the same package, to develop a stepwise regression model, which was selected based on the principle of minimal AIC (Akaike information criterion) among 1,000 iterations.

K-Nearest neighbors

The K-Nearest Neighbors algorithm relies on the proximity of the novel data point to the nearest neighbors in the training dataset to make decisions. In particular, for classification tasks, the algorithm identifies the class of a new data point by selecting the K closest neighbors based on distance. Hence, with the help of "kknn" package, we utilized 'train.kknn' function to construct the optimal model with a ks value of 15, and the kernel was selected as "rectangular".

Random forests

The random forest classifier is a powerful learning method that comprises multiple decision trees. It possesses several advantages, such as insensitivity towards missing or outlier values and consistent stability. As a result, it has been successfully implemented in image feature classification tasks. In the present study, we optimized the mtry parameter and determined 1 to be the optimal value. For the number of trees, we utilized the default value of 300. The package name is "randomForest".

Decision trees

We implemented the classification and regression tree function in the "rpart" package. This function facilitated the construction of decision trees, and the resulting tree included a root node placed at the top to indicate the most significant variable, along with decision nodes and terminal nodes that displayed classification percentages. We selected a decision tree as one of our algorithms for data evaluation, given its exceptional ability to handle varying types of data. We used 0.01 as the "cp" value with 2 as the "maxdepth" parameter.

Gradient boosting trees

In our study, we utilized "XGBoost" modeling based on the "xgboost" package, which proved to be highly effective due to its advanced capability to handle complex and diverse variables. We converted both the testing and training data into matrices, as "XGBoost" solely supports matrix-based model evaluations. We optimally chose "eta", "nrounds", "max_depth", "gamma", and "colsample_bytree" as 0.035, 250, 3, 0, 1, respectively.

Support vector machines

In this dataset, support vector machines were employed to tackle the problem of quadratic optimization, which resulted in the creation of optimal separating boundaries between data points. Support vector machines can accommodate both linear and nonlinear class boundaries, taking into account the support vector coordinates of each observation or variable. It was chosen as one of the algorithms to evaluate model performance due to its superior ability to capture the inherent characteristics of the data. We finally designed a "radial" support vector machine with 100 as the C parameter and 0.001 as the sigma parameter using the package named "e1071".

Multilayer perceptron

In this study, multi-layer perceptron-based artificial neural networks were utilized. This supervised learning technique incorporates a feed-forward structure comprised of input, hidden, and output layers. A neural network was selected for model assessment in this investigation due to its capacity to manage high data volatility. The best model had 13 neurons with 0.06 as the decay.

https://dx.doi.org/10.21037/qims-24-595

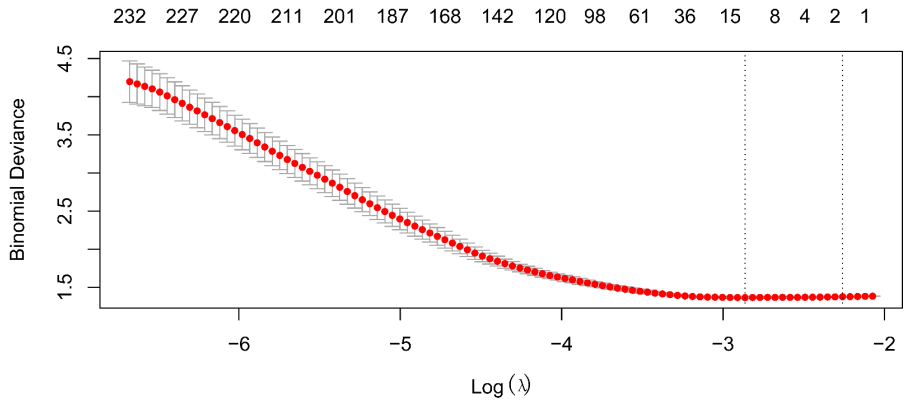

Figure S1 Searching for the best lambda for Lasso models based on binomial deviance.

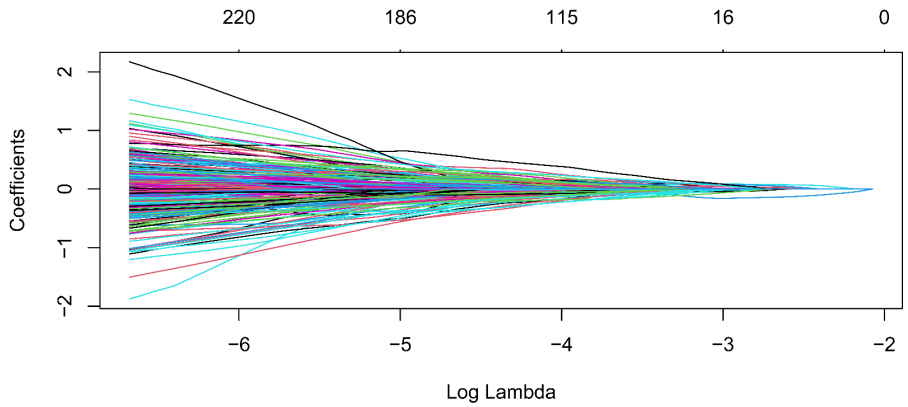

Figure S2 Coefficients alterations in different Lasso models with different lambda.

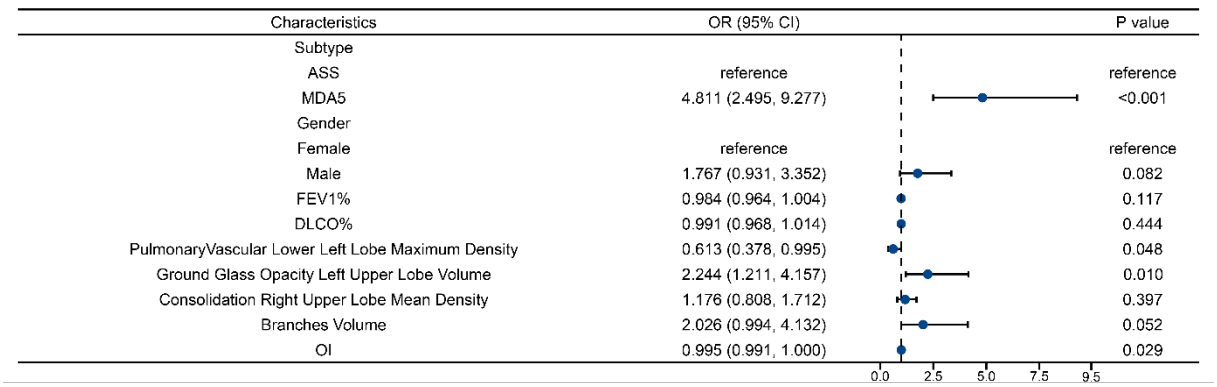

Figure S3 Effects of predicting factors included in the final model. OR, odd ratio; CI, confidence interval; ASS, antisynthetase syndrome; MDA5, melanoma differentiationassociated protein 5; FEV_1%, forced expiratory volume in 1 second as a percentage of the predicted value; DL_{CO}%, diffusing capacity of the lung for carbon monoxide as a percentage of the predicted value; OI, oxygenation index.

https://dx.doi.org/10.21037/qims-24-595

Table S1 Quantitative feature with non-zero Lasso coefficients

Class	Name	Coefficient
Pulmonary artery and vein	Vascular curvature	0.043842
Arteries	Maximum density (HU)	–0.00243
Veins	Blood volume at 5% of vascular diameter (mL)	–0.15156
Lung segment	Posterior segment R-S6 mean density (HU)	0.080865
	Supralingual segment L-S4-lung tissue volume (mL)	0.030311
	Supralingual segment L-S4-mass (g)	0.000595
Pulmonary fissure	Left lung oblique fissure-mean density (HU)	0.033987
	Right lung diastasis-mean curvature	0.070957
Lung density	Left lung-volume (mL)	0.043747
Pulmonary vasculature	Left lower lobe-maximum density (HU)	–0.01883
Ground glass	Upper left lobe-volume (mL)	0.006086
Consolidation	Right upper lobe-mean density (HU)	–0.03593
Bronchus	86-volume (mL)	0.025961
	92-volume (mL)	–0.03694

Lasso, least absolute shrinkage and selection operator; HU, Hounsfield unit.

https://dx.doi.org/10.21037/qims-24-595

Table S2 Comparison between train and test datasets using 514 patients

Class	Features	Overall	Train	Test	P
n		514	359	155	
Pulmonary artery and vein: median [IQR]	Vascular curvature	1.09 [1.07, 1.12]	1.09 [1.07, 1.12]	1.09 [1.08, 1.11]	0.816
Arteries: median [IQR]	Maximum density (HU)	562.50 [405.25, 768.75]	571.00 [405.50, 808.50]	542.00 [405.50, 702.50]	0.466
Veins: median [IQR]	Blood volume at 5% of vascular diameter (mL)	14.13 [9.46, 19.89]	14.55 [9.86, 20.08]	13.14 [8.71, 18.82]	0.043
Lung segment: median [IQR]	Posterior segment R-S6 mean density (HU)	−709.24 [−770.39, −636.09]	−710.23 [−768.84, −638.55]	−704.61 [−773.77, −631.28]	0.856
	Supralingual segment L-S4-lung tissue volume (mL)	29.85 [21.18, 41.14]	29.39 [21.00, 39.04]	31.54 [22.24, 45.03]	0.092
	Supralingual segment L-S4-mass (g)	31.05 [22.02, 42.79]	30.56 [21.84, 40.60]	32.81 [23.12, 46.83]	0.092
Pulmonary fissure: median [IQR]	Left lung oblique fissure-mean density (HU)	−688.92 [−764.14, −611.26]	−691.17 [−763.74, −614.90]	−687.50 [−767.67, −605.96]	0.703
	Right lung diastasis-mean curvature	0.79 [0.64, 0.98]	0.79 [0.65, 0.96]	0.81 [0.62, 1.01]	0.888
Lung density: median [IQR]	Left lung-volume (mL)	5.30 [1.40, 14.70]	5.65 [1.44, 15.72]	4.64 [1.36, 12.59]	0.218
Pulmonary vasculature: median [IQR]	Left lower lobe-maximum density (HU)	411.50 [275.25, 528.00]	420.00 [275.00, 535.50]	391.00 [276.00, 499.00]	0.272
Ground glass: median [IQR]	Upper left lobe-volume (mL)	5.58 [1.27, 18.27]	5.44 [1.15, 18.07]	6.06 [1.44, 21.76]	0.248
Consolidation: median [IQR]	Right upper lobe-mean density (HU)	−41.44 [−84.50, −8.61]	−39.88 [−82.47, −9.62]	−47.79 [−86.19, −8.32]	0.954
Bronchus: median [IQR]	86-volume (mL)	0.14 [0.07, 0.29]	0.14 [0.07, 0.29]	0.14 [0.06, 0.30]	0.864
	92-volume (mL)	0.14 [0.07, 0.27]	0.14 [0.07, 0.28]	0.14 [0.07, 0.26]	0.753
Status, n (%)					0.120
	Non-RP-ILD	265 (51.6%)	177 (34.4%)	88 (17.1%)	
	RP-ILD	249 (48.4%)	182 (35.4%)	67 (13.0%)	
Subtype, n (%)					0.186
	ASS	357 (69.5%)	243 (47.3%)	114 (22.2%)	
	MDA5+ DM	157 (30.5%)	116 (22.6%)	41 (8%)	
Gender, n (%)					0.467
	Female	367 (71.8%)	253 (49.5%)	114 (22.3%)	
	Male	144 (28.2%)	104 (20.4%)	40 (7.8%)	
Age, median (IQR)		54 (46, 61)	54 (47, 61)	55 (46, 62)	0.765
VC, median (IQR)		2.21 (1.75, 2.8425)	2.19 (1.745, 2.85)	2.26 (1.85, 2.75)	0.644
VC%, median (IQR)		73.20 (61.23, 85.05)	73.10 (60.00, 82.15)	76.70 (62.40, 90.00)	0.120
FVC, median (IQR)		2.18 (1.74, 2.82)	2.13 (1.72, 2.84)	2.26 (1.82, 2.75)	0.519
FVC%, median (IQR)		74.10 (62.33, 87.18)	73.45 (61.45, 84.40)	76.90 (64.15, 93.03)	0.123
FEV_1, median (IQR)		1.79 (1.41, 2.28)	1.77 (1.39, 2.28)	1.80 (1.47, 2.22)	0.763
FEV_1%, mean ± SD		72.56±18.11	71.70±17.67	74.71±19.08	0.174
FEV_1/FVC, median (IQR)		80.84 (76.48, 85.06)	81.35 (76.91, 86.01)	80.50 (76.04, 84.34)	0.164
TLC, median (IQR)		3.54 (2.90, 4.24)	3.50 (2.87, 4.25)	3.63 (2.97, 4.15)	0.742
TLC%, median (IQR)		70.40 (59.00, 81.20)	69.50 (58.85, 80.80)	71.60 (61.33, 82.75)	0.265
DL_{CO}, median (IQR)		4.57 (3.66, 5.58)	4.49 (3.66, 5.66)	4.67 (3.68, 5.46)	0.820
DL_{CO}%, median (IQR)		57.20 (45.90, 69.60)	56.20 (45.80, 69.25)	58.6 (46.15, 69.88)	0.761
FiO_2, median (IQR)		0.21 (0.21, 0.21)	0.21 (0.21, 0.21)	0.21 (0.21, 0.21)	0.520
PaO_2, median (IQR)		84.00 (74.80, 93.00)	84.00 (74.85, 92.45)	85.00 (74.20, 94.20)	0.529
$PaCO_2$, median (IQR)		37.10 (34.35, 40.30)	37.25 (34.50, 40.28)	37.00 (34.10, 40.90)	0.840
OI, median (IQR)		390.48 (342.86, 433.57)	389.52 (342.86, 429.29)	395.24 (342.86, 439.52)	0.540

For variables that obey normal distribution and have homogeneity of variance, we use a *t*-test. For variables that follow a normal distribution but do not have homogeneity of variance, we use Welch's *t*-test. For variables that do not follow a normal distribution, we use the Wilcoxon rank-sum test. RP-ILD, rapid progressive interstitial lung disease; ASS, anti-synthetase syndrome; MDA5+ DM, anti-melanoma differentiation-associated protein 5 dermatomyositis; VC, vital capacity; VC%, the proportion of actual value to the expected value for vital capacity; FVC, forced vital capacity; FVC%, the proportion of actual value to the expected value for forced vital capacity; FEV_1, forced expiratory volume in the first second; FEV_1%, the proportion of actual value to the expected value for forced expiratory volume in the first second; FEV_1/FVC, the proportion of forced expiratory volume in the first second to the forced vital capacity; TLC, total lung capacity; TLC%, the proportion of actual value to the expected value for total lung capacity; DL_{CO}, carbon monoxide diffusing capacity; DL_{CO}%, the proportion of actual value to the expected value for carbon monoxide diffusing capacity; FiO_2, fraction of inhaled oxygen; PaO_2, arterial oxygen pressure; $PaCO_2$, arterial carbon dioxide pressure; IQR, interquartile range; SD, standard deviation; HU, Hounsfield unit.

https://dx.doi.org/10.21037/qims-24-595

Table S3 Comparison between train and test datasets using 270 patients

Class	Features	Train	Test	P
n		190	80	
Pulmonary artery and vein: median (IQR)	Vascular curvature	1.09 (1.07, 1.12)	1.09 (1.07, 1.11)	0.626
Arteries: median (IQR)	Maximum density (HU)	581.00 (430.50, 934.50)	566.50 (412.75, 853.75)	0.636
Veins: median (IQR)	Blood volume at 5% of vascular diameter (mL)	13.74 (10.52, 19.26)	15.46 (10.22, 20.49)	0.283
Lung segment: median (IQR)	Posterior segment R-S6 mean density (HU)	–714.20 (–769.78, –635.54)	–700.01 (–751.39, –640.39)	0.573
	Supralingual segment L-S4-lung tissue volume (mL)	29.72 (21.18, 39.22)	31.26 (23.11, 42.88)	0.326
	Supralingual segment L-S4-mass (g)	30.91 (22.03, 40.79)	32.52 (24.03, 44.60)	0.326
Pulmonary fissure: median (IQR)	Left lung oblique fissure-mean density (HU)	–690.28 (–765.80, –621.57)	–698.15 (–763.68, –646.59)	0.799
	Right lung diastasis-mean curvature	0.78 (0.62, 0.96)	0.75 (0.59, 0.91)	0.718
Lung density: median (IQR)	Left lung-volume (mL)	5.24 (1.39, 15.62)	4.34 (1.10, 14.22)	0.691
Pulmonary vasculature: median (IQR)	Left lower lobe-maximum density (HU)	433.50 (279.25, 520.25)	403.50 (273.50, 551.00)	0.634
Ground glass: median (IQR)	Upper left lobe-volume (mL)	5.37 (1.39, 18.27)	3.83 (1.26, 11.42)	0.210
Consolidation: median (IQR)	Right upper lobe-mean density (HU)	–40.79 (–78.04, –7.69)	–34.28 (–68.53, –0.08)	0.347
Bronchus: median (IQR)	86-volume (mL)	0.12 (0.07, 0.29)	0.16 (0.08, 0.29)	0.367
	92-volume (mL)	0.14 (0.07, 0.25)	0.16 (0.08, 0.30)	0.498
RP, n (%)				0.968
	Non-RP-ILD	105 (38.9%)	44 (16.3%)	
	RP-ILD	85 (31.5%)	36 (13.3%)	
Subtype, n (%)				0.937
	ASS	141 (52.2%)	59 (21.9%)	
	MDA5+ DM	49 (18.1%)	21 (7.8%)	
Gender, n (%)				0.507
	Female	145 (53.7%)	58 (21.5%)	
	Male	45 (16.7%)	22 (8.1%)	
Age, median (IQR)		54.00 (47.00, 60.00)	57.00 (51.00, 62.00)	0.044
VC, median (IQR)		2.18 (1.75, 2.80)	2.23 (1.75, 2.84)	0.814
VC%, median (IQR)		73.25 (61.50, 82.40)	68.65 (62.00, 85.20)	0.771
FVC, median (IQR)		2.14 (1.74, 2.82)	2.20 (1.70, 2.77)	0.895
FVC%, median (IQR)		74.50 (62.78, 85.45)	70.25 (62.53, 88.03)	0.836
FEV_1, median (IQR)		1.75 (1.41, 2.28)	1.86 (1.41, 2.25)	0.856
FEV_1%, median (IQR)		73.90 (60.48, 81.80)	70.35 (62.00, 84.50)	0.971
FEV_1/FVC, median (IQR)		81.48 (76.72, 85.96)	80.76 (77.35, 84.98)	0.838
TLC, median (IQR)		3.48 (2.92, 4.15)	3.63 (2.86, 4.22)	0.782
TLC%, median (IQR)		71.15 (60.20, 80.53)	68.75 (57.75, 81.23)	0.573
DL_{CO}, median (IQR)		4.40 (3.55, 5.35)	4.64 (3.56, 5.57)	0.530
DL_{CO}%, mean ± SD		56.14±15.98	57.29±15.74	0.588
FiO_2, median (IQR)		0.21 (0.21, 0.21)	0.21 (0.21, 0.21)	0.058
PaO_2, median (IQR)		84.75 (77.00, 92.00)	84.50 (78.75, 92.13)	0.708
$PaCO_2$, median (IQR)		38.20 (35.53, 41.10)	37.15 (34.50, 40.65)	0.126
OI, median (IQR)		396.43 (359.76, 433.33)	400.24 (371.43, 438.10)	0.365

For variables that obey normal distribution and have homogeneity of variance, we use a *t*-test. For variables that follow a normal distribution but do not have homogeneity of variance, we use Welch's *t*-test. For variables that do not follow a normal distribution, we use the Wilcoxon rank-sum test. RP-ILD, rapid progressive interstitial lung disease; ASS, anti-synthetase syndrome; MDA5+ DM, anti-melanoma differentiation-associated protein 5 dermatomyositis; VC, vital capacity; VC%, the proportion of actual value to the expected value for vital capacity; FVC, forced vital capacity; FVC%, the proportion of actual value to the expected value for forced vital capacity; FEV_1, forced expiratory volume in the first second; FEV_1%, the proportion of actual value to the expected value for forced expiratory volume in the first second; FEV_1/FVC, the proportion of forced expiratory volume in the first second to the forced vital capacity; TLC, total lung capacity; TLC%, the proportion of actual value to the expected value for total lung capacity; DL_{CO}, carbon monoxide diffusing capacity; DL_{CO}%, the proportion of actual value to the expected value for carbon monoxide diffusing capacity; FiO_2, fraction of inhaled oxygen; PaO_2, arterial oxygen pressure; $PaCO_2$, arterial carbon dioxide pressure; IQR, interquartile range; SD, standard deviation; HU, Hounsfield unit.

https://dx.doi.org/10.21037/qims-24-595

Table S4 Description of initial treatment strategies between clinical subgroups

Characteristics	Overall	ASS	MDA5+ DM	P
n	514	357	157	
The time from respiratory symptom onset to treatment initiation (month), median (IQR)	0.83 (0.00, 3.12)	1.68 (0.00, 5.10)	0.02 (0.00, 0.98)	<0.001
Initial treatment strategy, n (%)				<0.001
Glucocorticoid	161 (38.42)	122 (45.69)	39 (25.66)	
Glucocorticoid + immunosuppressant (dual)	174 (41.53)	117 (43.82)	57 (37.50)	
Glucocorticoid + immunosuppressants (triple combination)	10 (2.39)	1 (0.37)	9 (5.92)	
Glucocorticoid + immunoglobulin	17 (4.06)	6 (2.25)	11 (7.24)	
Glucocorticoid + immunosuppressant(s) + immunoglobulin	55 (13.13)	21 (7.87)	34 (22.37)	
Glucocorticoid + biologics	2 (0.48)	0 (0.00)	2 (1.32)	
Initial antifibrotic therapy, n (%)	26 (6.18)	19 (7.06)	7 (4.61)	0.314

ASS, anti-synthetase syndrome; MDA5+ DM, anti-melanoma differentiation-associated protein 5 dermatomyositis; IQR, interquartile range.

Table S5 Characteristics of included patients with idiopathic inflammation myopathy in the trainset

Characteristics	nonRP-ILD	RP-ILD	P
n	177	182	
Subtype, n (%)			<0.001
ASS	144 (40.1%)	99 (27.6%)	
MDA5+ DM	33 (9.2%)	83 (23.1%)	
Gender, n (%)			0.046
Female	134 (37.5%)	119 (33.3%)	
Male	43 (12.0%)	61 (17.1%)	
Age, median (IQR)	54.00 (46.00, 59.00)	54.00 (47.75, 63.00)	0.163
VC, median (IQR)	2.31 (1.83, 3.01)	2.00 (1.65, 2.66)	0.004
VC%, median (IQR)	75.50 (64.85, 86.75)	68.20 (56.75, 78.80)	<0.001
FVC, median (IQR)	2.28 (1.81, 2.89)	1.96 (1.63, 2.61)	0.006
FVC%, median (IQR)	76.70 (65.53, 88.73)	69.30 (56.98, 81.03)	0.001
FEV_1, median (IQR)	1.83 (1.48, 2.40)	1.71 (1.34, 2.08)	0.010
FEV_1%, median (IQR)	75.65 (62.65, 84.00)	67.45 (56.00, 78.18)	0.002
FEV_1/FVC, median (IQR)	80.90 (76.17, 85.02)	81.83 (77.23, 87.40)	0.344
TLC, median (IQR)	3.61 (2.98, 4.42)	3.36 (2.77, 4.01)	0.022
TLC%, median (IQR)	72.45 (62.03, 83.05)	64.60 (55.20, 77.50)	0.002
DL_{CO}, median (IQR)	4.86 (3.93, 6.07)	4.11 (3.29, 5.07)	<0.001
DL_{CO}%, median (IQR)	61.70 (51.43, 71.68)	50.20 (42.20, 61.00)	<0.001
FiO_2, median (IQR)	0.21 (0.21, 0.21)	0.21 (0.21, 0.21)	<0.001
PaO_2, median (IQR)	87.00 (80.00, 93.00)	81.00 (72.18, 92.00)	0.001
$PaCO_2$, mean ± SD	38.00±4.11	36.93±4.85	0.048
OI, median (IQR)	409.52 (376.55, 438.10)	368.53 (315.17, 422.38)	<0.001

For variables that obey normal distribution and have homogeneity of variance, we use a *t*-test. For variables that follow a normal distribution but do not have homogeneity of variance, we use Welch's *t*-test. For variables that do not follow a normal distribution, we use the Wilcoxon rank-sum test. RP-ILD, rapid progressive interstitial lung disease; ASS, anti-synthetase syndrome; MDA5+ DM, anti-melanoma differentiation-associated protein 5 dermatomyositis; VC, vital capacity; VC%, the proportion of actual value to the expected value for vital capacity; FVC, forced vital capacity; FVC%, the proportion of actual value to the expected value for forced vital capacity; FEV_1, forced expiratory volume in the first second; FEV_1%, the proportion of actual value to the expected value for forced expiratory volume in the first second; FEV_1/FVC, the proportion of forced expiratory volume in the first second to the forced vital capacity; TLC, total lung capacity; TLC%, the proportion of actual value to the expected value for total lung capacity; DL_{CO}, carbon monoxide diffusing capacity; DL_{CO}%, the proportion of actual value to the expected value for carbon monoxide diffusing capacity; FiO_2, fraction of inhaled oxygen; PaO_2, arterial oxygen pressure; $PaCO_2$, arterial carbon dioxide pressure; IQR, interquartile range; SD, standard deviation.

https://dx.doi.org/10.21037/qims-24-595

Table S6 Characteristics of included patients with idiopathic inflammation myopathy in the test set

Characteristics	RP-ILD	Non-RP-ILD	P
n	67	88	0.402
Subtype, n (%)			
MDA5+ DM	20 (12.9%)	21 (13.5%)	
ASS	47 (30.3%)	67 (43.2%)	0.182
Gender, n (%)			
Female	46 (29.9%)	68 (44.2%)	
Male	21 (13.6%)	19 (12.3%)	0.123
Age, mean ± SD	55.58 ± 12.20	52.59 ± 11.66	0.280
VC, median (IQR)	2.26 (1.77, 2.60)	2.35 (1.86, 2.92)	0.009
VC%, mean ± SD	69.33 ± 20.61	79.99 ± 17.21	0.155
FVC, median (IQR)	2.20 (1.70, 2.60)	2.37 (1.85, 2.94)	0.005
FVC%, mean ± SD	70.30 ± 21.39	82.07 ± 17.87	0.088
FEV_1, median (IQR)	1.75 (1.35, 2.05)	1.94 (1.50, 2.38)	0.003
FEV_1%, mean ± SD	67.13 ± 21.36	79.01 ± 16.34	0.314
FEV_1/FVC, mean ± SD	79.64 ± 6.43	80.91 ± 5.47	0.080
TLC, mean ± SD	3.42 ± 0.78	3.76 ± 0.95	0.009
TLC%, mean ± SD	66.72 ± 17.02	76.15 ± 15.49	0.055
DL_{CO}, mean ± SD	4.23 ± 1.19	4.83 ± 1.55	0.007
DL_{CO}%, mean ± SD	51.78 ± 13.89	61.52 ± 17.11	0.009
FiO_2, median (IQR)	0.21 (0.21, 0.21)	0.21 (0.21, 0.21)	<0.001
PaO_2, median (IQR)	78.50 (68.75, 88.33)	90.00 (81.20, 98.00)	0.032
$PaCO_2$, median (IQR)	35.25 (33.25, 40.45)	38.00 (35.20, 41.10)	<0.001
OI, median (IQR)	342.86 (301.55, 405.95)	423.81 (376.19, 461.90)	<0.001

For variables that obey normal distribution and have homogeneity of variance, we use a *t*-test. For variables that follow a normal distribution but do not have homogeneity of variance, we use Welch's *t*-test. For variables that do not follow a normal distribution, we use the Wilcoxon rank-sum test. RP-ILD, rapid progressive interstitial lung disease; ASS, anti-synthetase syndrome; MDA5+ DM, anti-melanoma differentiation-associated protein 5 dermatomyositis; VC, vital capacity; VC%, the proportion of actual value to the expected value for vital capacity; FVC, forced vital capacity; FVC%, the proportion of actual value to the expected value for forced vital capacity; FEV_1, forced expiratory volume in the first second; FEV_1%, the proportion of actual value to the expected value for forced expiratory volume in the first second; FEV_1/FVC, the proportion of forced expiratory volume in the first second to the forced vital capacity; TLC, total lung capacity; TLC%, the proportion of actual value to the expected value for total lung capacity; DL_{CO}, carbon monoxide diffusing capacity; DL_{CO}%, the proportion of actual value to the expected value for carbon monoxide diffusing capacity; FiO_2, fraction of inhaled oxygen; PaO_2, arterial oxygen pressure; $PaCO_2$, arterial carbon dioxide pressure; SD, standard deviation; IQR, interquartile range.

https://dx.doi.org/10.21037/qims-24-595